ARMA 19–1981

Well integrity of high temperature wells: Effect of mineralogical changes on mechanical properties of well cement

TerHeege, J.H. and Wollenweber, J.
TNO Applied Geosciences, Utrecht, the Netherlands
Marcel Naumann
Equinor ASA, Sandsli, Norway
Pipilikaki, P.
TNO Structural Reliability, Delft, the Netherlands
Vercauteren, F.
TNO Material Solutions, Eindhoven, the Netherlands

ABSTRACT: Wells used for steam-assisted gravity drainage (SAGD), for cyclic steam stimulation (CSS), for hydrocarbon production in areas with anomalous high geothermal gradient, or for geothermal energy extraction all are operated in high temperature environments where maintaining long term wellbore integrity is one of the key challenges. Changes in cement mineralogy and associated mechanical properties may critically affect the integrity of high temperature wells. In this study, the relation between changes in mineralogy and mechanical properties of API class G cement with 40% silica flour was investigated by exposing samples for 1-4 weeks to temperatures of 60-420°C. The effect of mineralogical changes on mechanical properties was investigated using a combination of chemical and microstructural analysis and triaxial strength tests at confining pressures of 2-15 MPa. The combined effect of changing porosity, microstructure and strength of mineral phases determines changes in mechanical behavior, in particular the formation of stronger mineral phases with higher density affect Young's modulus, failure strength and residual strength. Deformation of the cement is more brittle at low confining pressures and more ductile at high confining pressures with a considerable residual strength after failure and highest reduction in cement stiffness and increase in strength at temperatures of ~250°C.

1. INTRODUCTION

Wells that are drilled or operated in high temperature environments can be subject to higher risks of losing integrity and zonal isolation. Examples of such high temperature wells include wells used for steam-assisted gravity drainage (SAGD) or for cyclic steam stimulation (CSS), wells drilled in areas with anomalous high geothermal gradient (HPHT wells), or geothermal wells (Stiles, 2006; Chartier et al., 2015; Frioleiffson et al., 2015). Maintaining long term wellbore integrity in these situations is one of the key challenges determining the technical and commercial success of projects that require wells to operate at high temperatures.

Changes in cement mineralogy and associated mechanical properties critically affect the integrity of high temperature wells. Standard cement formulations have been reported to reach their mechanical and chemical (stability) limits due to the harsh conditions and extreme cyclic temperature loads in high temperature (HT) and high pressure (HP) wells (Enform, 2012; Chartier et al., 2015). For standard curing conditions, hydration of ordinary Portland cement (OPC, e.g., class G well cement) with a calcium oxide to silicon dioxide (C/S) ratio close to 3.1 produces the amorphous C-S-H and the crystalline $Ca(OH)_2$. The product is a mixture of ordered and disordered phases with C-S-H present as a highly disordered version of the crystalline tobermorite and jennite phases (Taylor, 1990). Tobermorite preserves high compressive strength and low permeability. Mineralogical and mechanical changes are expected to occur in OPC above ~110°C (Thorvaldson et al., 1938; Patchen, 1960; Taylor, 1990; Kyritsis et al., 2009). Reactions result in different hydration products, i.e. crystallization of alpha dicalcium silicate hydrate (α-C_2SH or $Ca_2SiO_3(OH)_2$) is favored. The lime-rich alpha-dicalcium silicate hydrate (α-C_2SH) is denser than the usual calcium silicate hydrate (C-S-H gel) product. Bulk volume decrease, and cement shrinkage or porosity increase is associated with this reaction, which results in a decrease in cement strength and increase in permeability

(Patchen, 1960; Pernites and Santra, 2016). All types of OPC and other types of well cements with similar composition show lower strengths when cured above 110°C, compared to curing at 93°C.

Elevated curing temperatures are commonly reached by SAGD, CCS, HPHT oil and gas wells or geothermal wells in areas with moderate to high geothermal gradients. Changes in cement properties need to be accounted for in the design of cement formulations as well as cementation procedures of these wells to ensure the plugging of loss zones during drilling, proper anchoring, corrosion protection of casing strings, zonal isolation and well integrity at elevated temperatures and pressures (HPHT conditions). A common practice is to use Portland-type cements with added silica (such as fly ash, silica fume or quartz flour) to stabilize cement at higher temperature. Reactions of $Ca(OH)_2$ with added silica at elevated temperatures result in a C-S-H with a lower C/S ratio. Addition of 35 to 40% by weight of cement is enough to prevent the reaction forming α-C_2SH. Instead, cement phases such as tobermorite or xonotlite are formed (Patchen, 1960). Moreover, for a water to solids ratio of 0.4, a formulation with added silica results in 91% of the water being chemically bound against only 39 % of the available water in the OPC. Addition of ~40% silica flour thereby favors formation of high strength and low permeability mineral phases.

Despite the importance for well integrity of high temperature wells, data on mineralogical and mechanical changes during exposure of well cements to HPHT conditions is limited. Some relevant laboratory studies are available (Taylor 1990; Gabrovšek et al., 1993; Meller et al., 2009; Pernites and Santra, 2016), but investigations of the relation between mineralogical and mechanical changes at different exposure times and temperatures are sparse. In this study, the relation between changes in mineralogy and mechanical properties of API class G cement with 40% silica flour was investigated. Samples were exposed to temperatures of 60°C (curing only) up to 420°C (curing and exposure) for exposure times of 3 days (curing time) to 4 weeks (HT exposure). The effect of mineralogical changes on mechanical properties was investigated using a combination of (1) chemical analysis using X-ray diffraction (XRD), (2) microstructural analysis using scanning electron microscopy (SEM) and optical microscopy, and (3) mechanical properties (Young's modulus, failure stress, residual stress) using triaxial tests at confining pressures of 2-15 MPa.

Results show that the formation of high temperature mineral phases in the cement such as tobermorite, xonotlite and wollastonite is associated with marked changes in elastic properties and failure behavior. Critical conditions for the changes in mechanical behavior are determined, and the implications for well integrity and design of new cement formulations are discussed. The findings aid in assessing risks of well integrity loss and mitigation of these risks by designing new cement formulations. The main challenge remains to optimize cement properties for prolonging the integrity of cement at high temperatures while maintaining low viscosity of cement slurry during well cementation.

2. EXPERIMENTAL APPROACH

2.1. Sample material

Synthetic cement samples, Dyckerhoff HT Basic Blend of cement clinker (API class G cement) with 40 % silica flour was used as a starting material (Papaioannou, 2018). Specimens are prepared using the Dyckerhoff blend and demineralized water with a water to solid (cement + silica flour) ratio of 0.371 (m/m). For the mixing process, the EN 196-3 protocol was followed. After each step the weight of the samples was checked for dehydration. After mixing, the slurry was injected into cylindrical molds with 25 mm internal diameter and 60 mm length using a 10 ml syringe in order to achieve homogeneity and minimize air entrapment. The molds were subsequently sealed to prevent water evaporation, and exposed for 72 hours at 60°C and atmospheric pressure in a furnace. Samples exposed to 120, 250 and 420°C were subsequently cooled down for 2 hours before demolding. Pressure resistant glass bottles were used for exposure of pairs of samples under suspension of water at 120°C and 2 bar in a furnace. Metal sample holders sealed by a cap with two different types of O-rings were used with a pre-defined amount of water to obtain required exposure conditions. Samples exposed to 60 and 120°C were cooled down in two hours, while for samples exposed to 250 and 420°C samples a 3 day gradual cooling protocol was applied. For mineralogical and microstructural analysis, samples were exposed for 4 weeks to 60, 120, 250 and 420°C. For the triaxial experiments, samples were cut and manually polished to obtain samples with plane parallel surfaces, a final length between 49.6 and 52.2 mm, and a final diameter between 24.6 and 25.0 mm. Samples were tested after curing ("cured only" samples), or after exposure of 1 week to 120°C at 2 bars, 4 weeks to 250°C at 40 bars, and 2 weeks to 420°C at 350 bars, respectively.

2.2. Mineralogical and microstructural analysis

Analysis of mineral phases in the samples was performed using X-ray diffraction (XRD) and energy dispersive X-ray spectroscopy (EDX). Microstructural analysis was performed using optical microscopy and scanning electron microscopy (SEM).

XRD analysis was performed on grinded aliquots to access the crystalline compounds and deterioration products. Quantitative analysis was performed on samples exposed for 4 weeks to 60, 120 and 420°C (2 samples, Table 1). Mineralogy of samples exposed for 4

weeks to 250°C was analyzed on the basis of a XRD spectrum of one sample. Samples were measured in Bragg-Brentano geometry with a Bruker D8 Advance diffractometer, equipped with a motorized slit with opening angle of 0.30°, primary and secondary soller slit of 2.5° and Lynxeye detector with opening angle of 2.94° and Ni-Kß filter. Data collection was carried out at room temperature using Cu Kα radiation (λ = 0.15406 nm) in the 2θ region between 10° and 120°, step size 0.015 degrees 2θ. The sample was deposited on a zero background holder (Si single crystal <510> wafer) and was rotated at 15 rpm during the measurement. Generator settings were 40 kV and 40 mA.

For optical microscopy analysis, thin sections of the cement samples were prepared by sawing specimens of 50 × 30 × 15 mm (length × width × thickness) from each of the samples. The sawn specimens were slowly dried at 20ºC and subsequently impregnated under vacuum with an epoxy resin containing a fluorescent dye. After hardening of the resin, a thin section with a thickness of about 25 µm was prepared prism by grinding and polishing. Impregnation of the specimens with a fluorescent resin allows thin sections to be studied with both transmitted-light and fluorescent-light microscopy. The thin sections were examined with a LEICA optical microscope.

The SEM used in this investigation is a FEI NovaNanoSEM 650. The SEM was operated at an acceleration voltage of 5 kV in low (40 Pa) vacuum mode to avoid charging of the non-conductive specimen. The gaseous analytical solid-state, back-scattered electron detector (GAD) was used for imaging both topographic and material contrast. The same thin sections as used for optical microscopy were analyzed. The SEM is equipped with a Noran micro analysis system (EDX) for analyzing chemical composition. EDX analysis was performed on bulk material and specimens with a size down to approximately 1 µm.

2.3. Triaxial experiments

The triaxial experiments were conducted at confining pressures of 2-15 MPa, room temperature and pore pressures at ambient conditions. Samples were tested at initially fully saturated pore fluid conditions. Slow axial strain rate on the order of 5.10^{-6} s^{-1} were used to remain in drained conditions such that no excessive pore pressure is built-up internally. The triaxial cell allows for independent control of axial and radial stresses (confinement). Confining pressure is controlled via an external pump. The setup and procedure follow largely the suggested method for determining the strength of rock materials in triaxial compression (Kovari et al., 1983). Axial strains were measured indirectly by means of an external linear variable differential transformer (LVDT) only, implying that the combined displacement due to both sample deformation and load-dependent elastic shortening of the piston assembly is recorded. Therefore, axial strains measured in this setup are likely overestimated, possibly leading to an apparent lower sample stiffness (Young's modulus). Radial strains were not measured. Axial stress was measured by two load cells, located both inside and outside the pressure vessel.

Triaxial tests were conducted by hydrostatic loading of samples to predefined confinement, and subsequent triaxial compression at constant displacement rate until reaching an approximately constant plateau of post-failure (residual) stress. In two tests (GWL005 and GWL007), triaxial compression at constant displacement rate was initially to an axial stress of about 1/3 to 1/2 of expected peak stress, followed by triaxial unloading to initial stress conditions and re-loading until reaching an approximately constant plateau of post-failure (residual) stress at the same displacement rate.

The triaxial experiments were used to determine mechanical parameters (static Young's modulus, failure and residual strength) as function of stress state (confinement), specimen exposure temperature and duration.

3. RESULTS

3.1. Mineralogy

Samples cured for 4 weeks at 60°C mainly consist of hydration products ettringite, portlandite and katoite, amorphous hydrate phase and clinker phases C_3S and brownmillerite that have not completely reacted (Table 1).

Table 1. Mineralogical composition of samples exposed for 4 weeks at different temperatures determined by XRD analysis.

Mineral phase	60°C	120°C	420°C*
Ettringite	1.4	-	-
Portlandite	8.5	-	-
Katoite	3.5	2.6	-
C_3S	3.8	-	-
Brownmillerite	7.7	5.0	-
Tobermorite	-	10.4	-
Afwillite	-	0.6	-
α-C_2S hydrate	-	1.2	-
Quartz	26.2	13.1	-
Xonotlite	-	-	33.8-35.3
Wollastonite	-	-	14.8-15.9
Gypsum	-	-	1.1-2.4
Calcite	-	-	0.3
Amorphous content	48.9	67.1	46.1-49.9

*Range from measurement of two different samples.

Samples exposed for 4 weeks to 120°C mainly consist of hydration phases tobermorite, α-C_2S hydrate and afwillite. The clinker phase C_3S as well as the hydration products ettringite and portlandite have disappeared

completely at these conditions, while brownmillerite and katoite are detected in smaller amounts. Dissolution of quartz occurs, but reactions involving quartz are limited. The amount of metastable high Ca/Si ratio amorphous phases increases. Xonotlite is the main mineral phase that appears in samples exposed for 4 weeks to 250°C, accompanied by small amount of calcite. All other phases including cement hydrates, quartz and non-hydrated cement have disappeared. Samples exposed for 4 weeks to 420°C still mainly consist of xonotlite, but wollastonite, calcite and gypsum are also formed. The amorphous content decreased again compared to the samples exposed for 4 weeks at lower temperatures (Table 1).

3.2. Microstructure

Microstructures of samples cured for 4 weeks at 60°C show a very fine grained to amorphous matrix with areas of high and low porosity and large inhomogeneity of pore structure and water distribution in the sample (Fig. 1). Both darker areas with dense C-S-H cement grains and

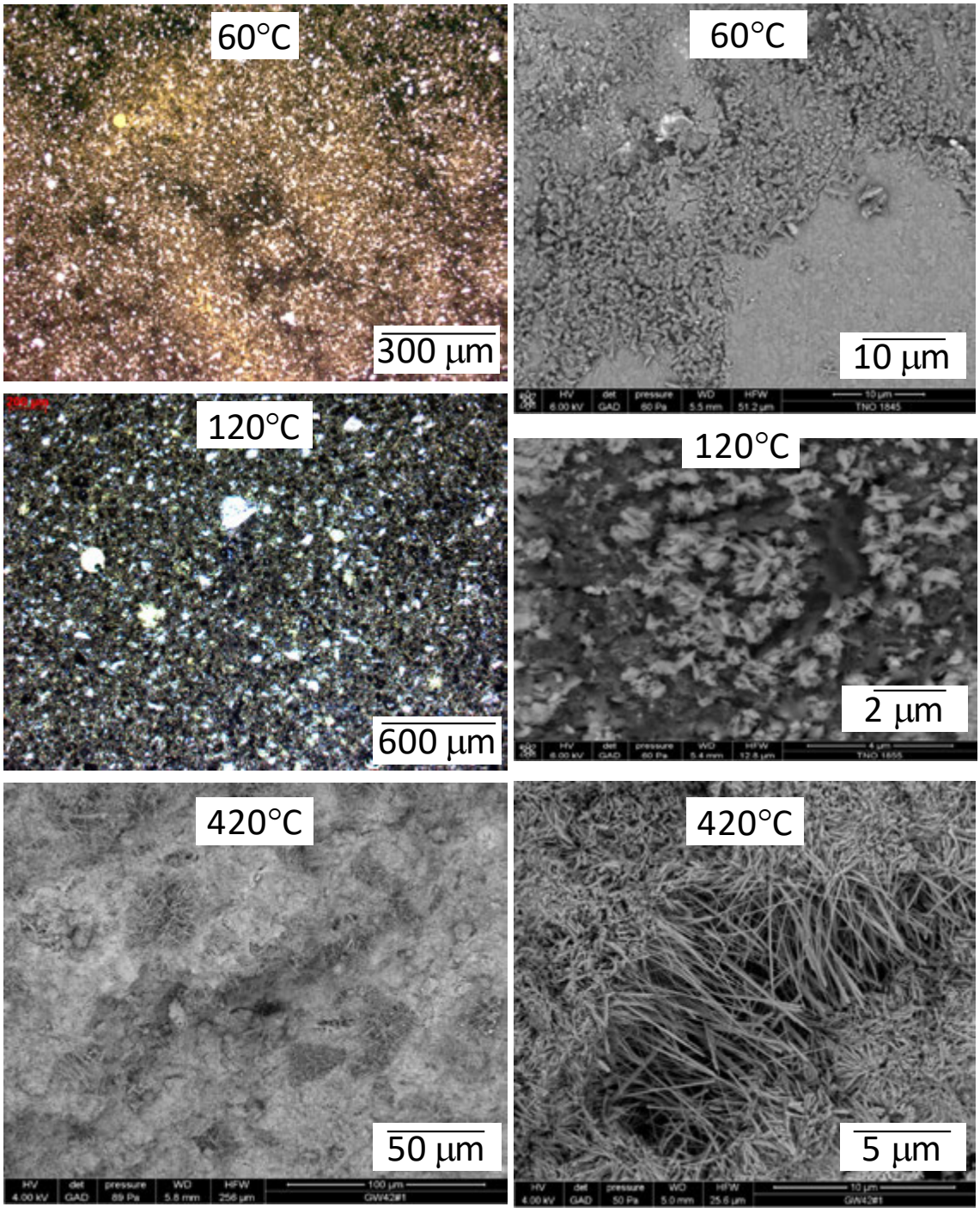

Fig. 1. Microstructures of samples exposed for 4 weeks to 60-420°C. Upper and middle left- light microscopy, others- scanning electron microscopy. See text for description of phases.

lower capillary porosity, and lighter areas with higher capillary porosity are present indicating local separation of water and micro-bleeding. The microstructure and distribution of capillary porosity of samples cured for 4 weeks at 120°C is more homogeneous than in the samples exposed to 60°C with similar porosity throughout the sample. A reaction front is observed between the C-S-H gel and the surrounding amorphous silica, and well-formed tobermorite crystals appear to grow inside the C-S-H gel. The microstructure of samples cured for 4 weeks at 420°C show needle-shaped crystals (probably wollastonite) cover the whole sample with longer crystals forming inside pre-existing voids and pores causing a reduction of porosity. Other (mainly amorphous phases) contain a relatively high amount of Fe, causing a reddish discoloring in some samples.

3.3. Mechanical behavior

Cured only samples have a Young's modulus (E) that increases from 4.9 GPa at 2 MPa confining pressure (P_c) to 9.5 MPa at P_c = 15 MPa (Table 2, Figure 2). A similar increasing trend of Young's modulus with confining pressure is observed for samples exposed for 1 week to 120°C (E = 6.4 GPa for P_c = 2 MPa to E = 7.5 GPa for P_c = 10 MPa). Compared to cured only samples, Young's modulus is increasing for P_c = 2 and 5 MPa, and decreasing for P_c = 10 MPa. The trend of increasing Young's modulus with increasing confining pressure is reversed for samples exposed for 4 weeks to 250°C and for 2 weeks to 420°C. Young's modulus is increasing if samples are exposed for 1 week to 120°C, at least for low confining pressures.

Table 2. Mechanical data from triaxial experiments.

Sample	Exposure	P_c MPa	σ_p MPa	σ_r MPa	E GPa
GWL003	Cured only	2	49.3	19.3	4.9
GWL005	Cured only	2	57.4	33.1	8.2
GWL011	Cured only	2	58.1	28.2	7.2
GWL004	Cured only	5	61.4	38.5	5.8
GWL002	Cured only	10	69.1	54.5	7.8
GWL009	Cured only	10	61.5	17.6	6.5
GWL006	Cured only	15	80.1	75.1	9.5
GWL012	1 week, 120°C	2	52.3	32.9	6.4
GWL013	1 week, 120°C	5	54.9	38.7	7.0
GWL007	1 week, 120°C	10	75.1	56.3	7.5
GWL018	4 weeks, 250°C	2	29.5	18.3	4.8
GWL014	4 weeks, 250°C	5	31.3	26.4	3.9
GWL019	4 weeks, 250°C	5	34.5	31.2	4.6
GWL016	2 weeks, 420°C	2	57.6	29.3	6.7
GWL015	2 weeks, 420°C	5	48.2	31.5	5.6
GWL017	2 weeks, 420°C	10	58.0	47.1	5.8

For longer exposures or higher exposure temperatures Young's modulus is mostly decreasing with increasing exposure time and exposure temperature. One exception is a sample exposed for 2 weeks to 420°C tested at P_c = 2 MPa, which shows a higher Young's modulus compared to cured only samples or samples exposed to 120°C.

The maximum (peak) differential stress (σ_p or failure strength) and (residual) differential stress after failure (σ_r or residual strength) increases with confining pressure in almost all samples (Table 2, Fig. 3). Failure strengths of

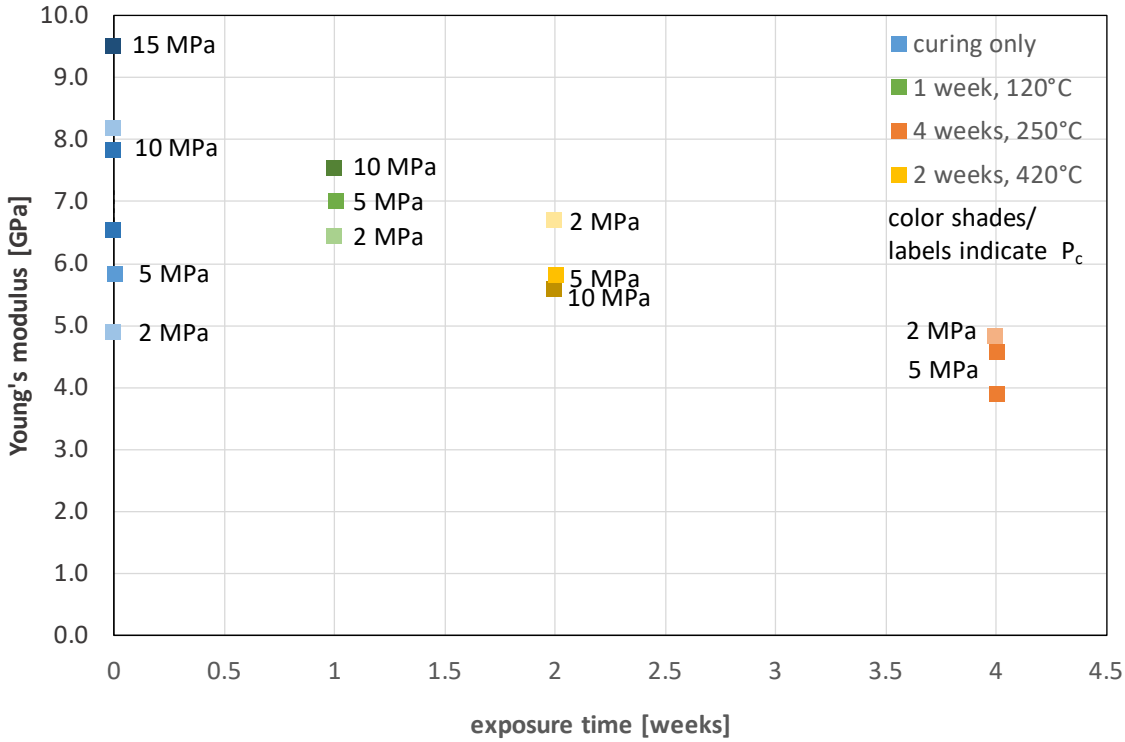

Fig. 2. Young's modulus of "cured only" samples and samples exposed for 1-4 weeks to 120-420°C.

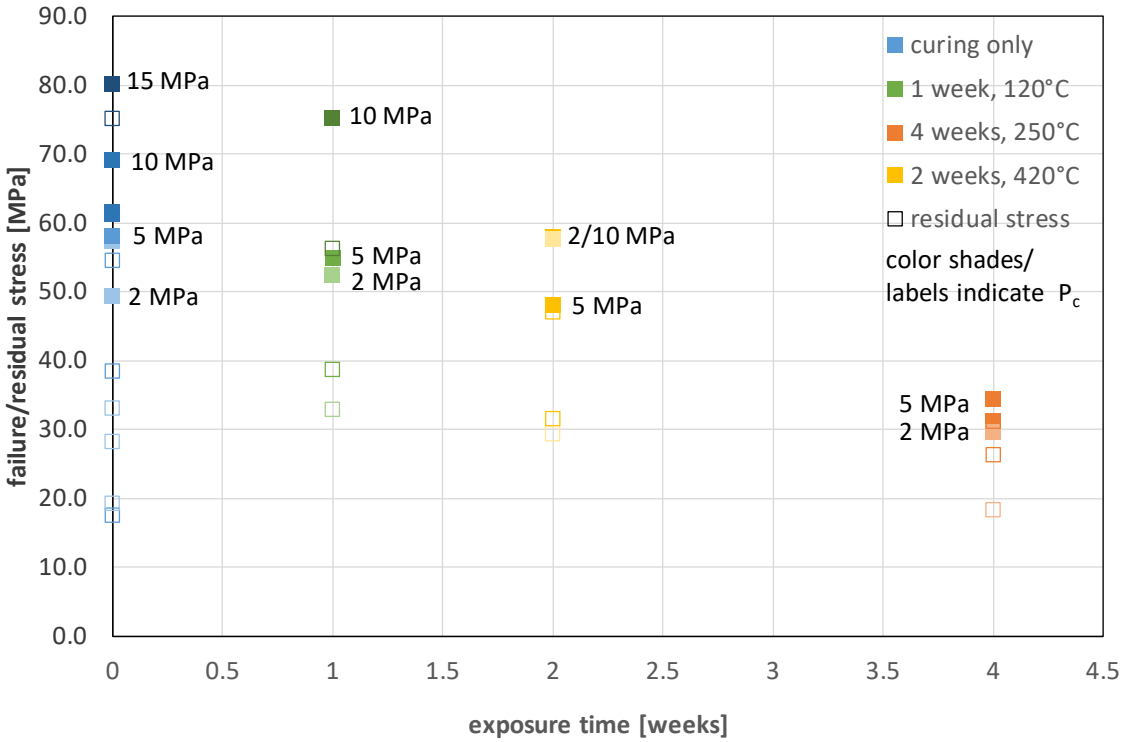

Fig. 3. Failure and residual strength of "cured only" samples and samples exposed for 1-4 weeks to 120-420°C.

the cured only samples are 49.3-58.1 MPa at P_c = 2 MPa to 80.1 MPa at P_c = 15 MPa. One sample exposed for 2 weeks to 420°C has similar failure strength for P_c = 2 MPa and 10 MPa, but its residual strength shows the general trend of increasing strength with increasing confining pressure. Trends of failure and residual strength with exposure time and temperature are comparable to the trends observed for Young's modulus, i.e. overall failure and residual stresses decrease with increasing exposure time and exposure temperature. Samples exposed for 1 week to 120°C have strengths that are comparable to the cured only samples. The relation between principal stresses (σ_1, σ_3) at failure (Fig. 4) suggest (1) a similar friction coefficient for samples exposed up to 250°C, (2) a change in friction coefficient with increasing exposure temperature between 250 and 420°C, and (3) a drop in uniaxial compressive strength (UCS) with exposure temperatures increasing from 120 to 250°C, followed by an increasing UCS between 250 and 420°C. Note that $\sigma_1 = C_0 + q\sigma_3$, with C_0 the uniaxial compressive strength and q related to the friction coefficient for a Mohr-Coulomb failure criterion (Al-Ajm and Zimmerman, 2005). The difference between failure and residual strength (Fig. 5) suggest a change from more brittle deformation at low confining pressures (i.e. a large stress drop after failure or large difference in strength) to more ductile deformation at high confining pressures (i.e. a small stress drop after failure that is spread out over larger axial strain).

The relative effect of exposure time and temperature on mechanical behavior is unclear. Further experiments on samples need to be performed to systematically explore these effects (for examples samples exposed for 2 weeks to 250°C or for 4 weeks to 420°C).

4. DISCUSSION

The relation between mineralogy, microstructure and mechanical behavior was investigated for cement samples consisting of Dyckerhoff HT Basic Blend of cement clinker (API class G cement) with 40% added silica flour. Previous studies showed that addition of 35 to 40% by weight of cement is enough to prevent the reaction forming α-C_2SH, and favor formation of stronger mineral phases such as tobermorite or xonotlite (Patchen, 1960). Addition of ~40% silica flour is therefore expected to favor formation of high strength and low permeability mineral phases at high temperatures, thereby improving cement stability and well integrity in high temperature wells.

The current study shows that deformation of the cement is more brittle deformation at low confining pressures and more ductile deformation at high confining pressures. The relation between mineralogy, microstructure and mechanical behavior is complex. Mineralogical changes occurring between curing at 60 and 120°C mostly result in slightly stiffer (i.e. higher Young's modulus) and stronger (i.e. higher failure and residual strength) cement. Cement becomes less stiff and weaker if temperatures are raised to 250°C. It becomes stiffer and stronger again if temperatures are further increased to 420°C. The observed changes may also be affected by exposure times, which have not been systematically varied.

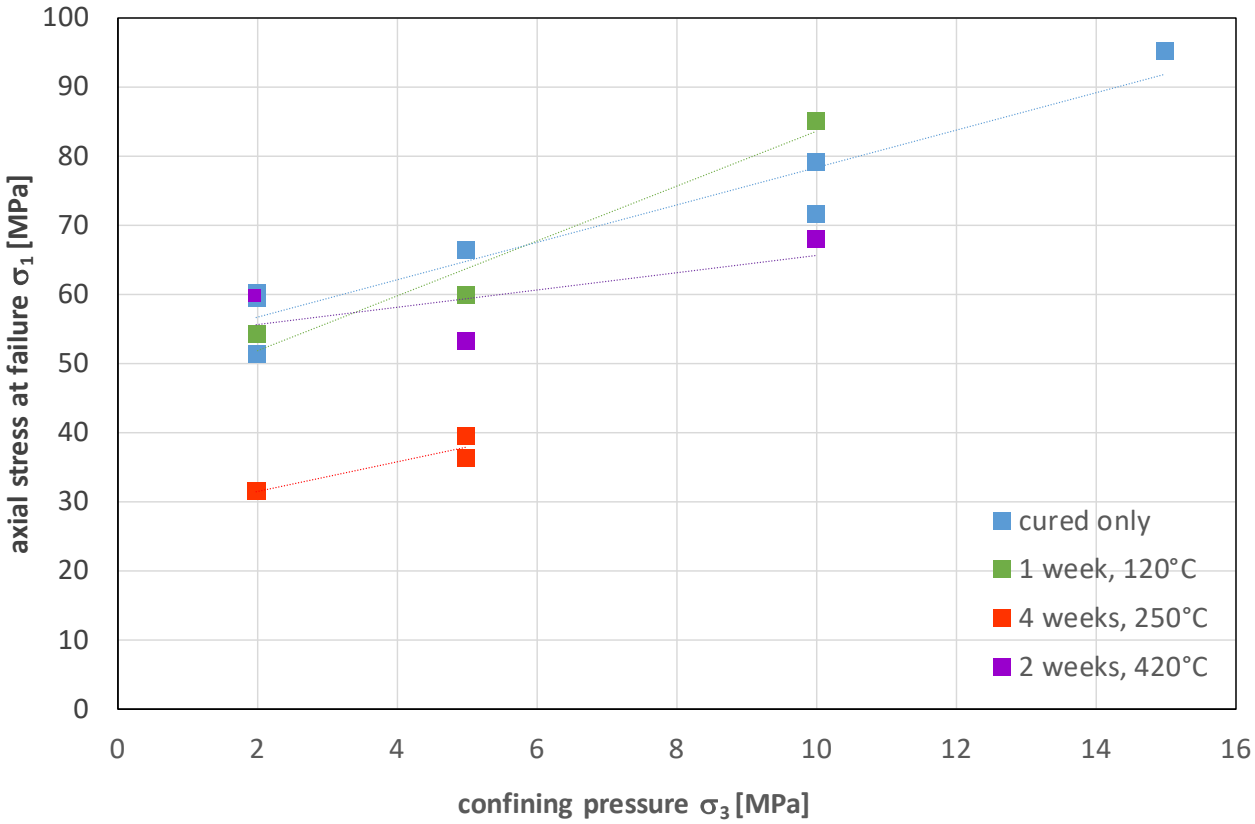

Fig. 4. Relation between the maximum principal stress (σ_1) at failure and minimum principal stress ($\sigma_3 = P_c$) of "cured only" samples and samples exposed for 1-4 weeks to 120-420°C. Best fit linear trends are also indicated (dashed lines).

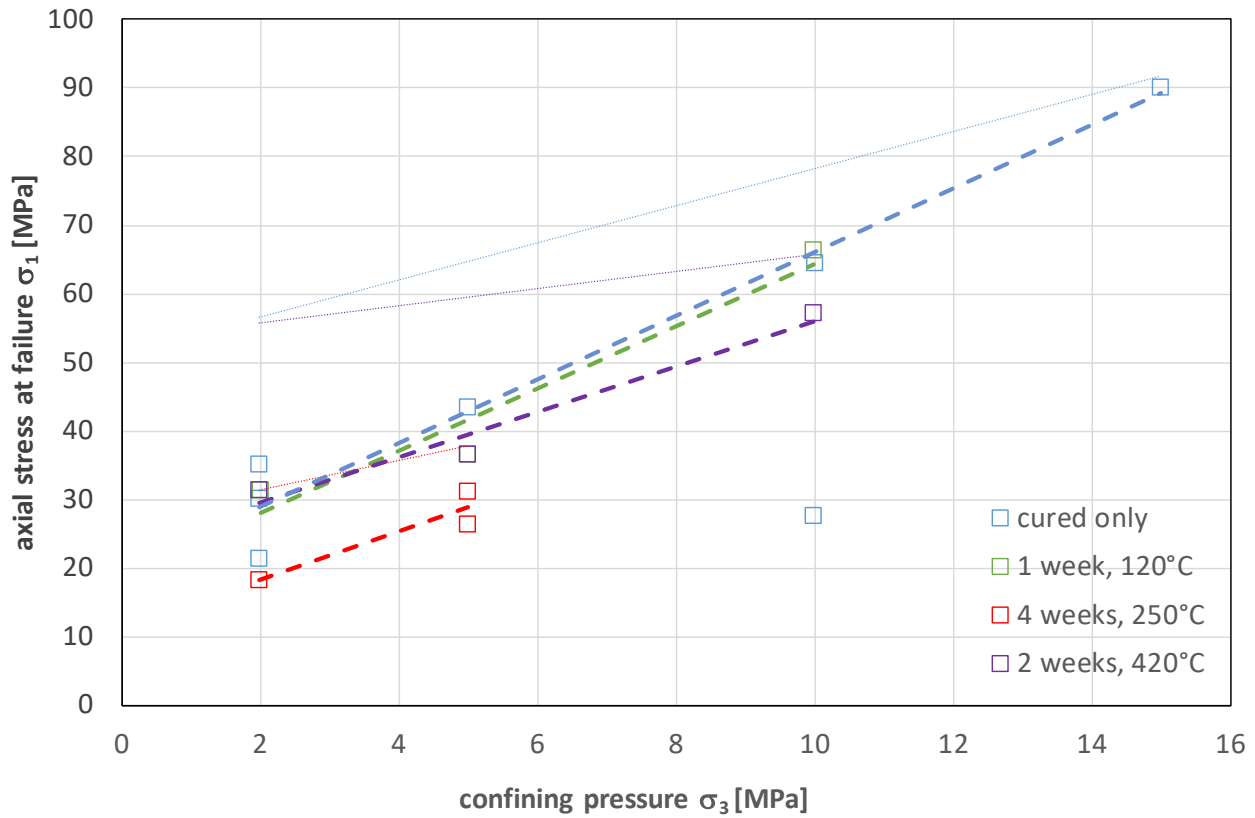

Fig. 5. Relation between the maximum principal stress (σ_1) at post failure residual strength and minimum principal stress ($\sigma_3 = P_c$) of "cured only" samples and samples exposed for 1-4 weeks to 120-420°C. Best fit linear trends are also indicated (dashed lines).

Comparison with other studies (Enform, 2012; Papaioannou 2018) and mineralogical observations (i.e. formation of stronger mineral phases) suggest that (1) samples may become stiffer and stronger for longer exposures at 120°C, and (2) stiffness and strength will further increase for longer exposure to 420°C.

The change in mechanical behavior is likely due to the combined effect of changing porosity, microstructure and strength of mineral phases, i.e. (1) formation of stronger xonotlite and wollastonite phases with higher density at the expense of tobermorite, α-C_2S hydrate, afwillite, brownmillerite and katoite (absent after exposure for 4 weeks at 420°C) and change in amorphous content (Table 1), (2) change in porosity due the different volume of reaction products, and (3) different microstructure (i.e. voids filled with needle-shaped crystals).

The most important issue with this complex relation between mineralogical, microstructural and mechanical changes in this high temperature cement is with the reduction in stiffness and strength around ~250°C. Young's modulus can drop by 25-44% between 120°C and 250°C within weeks of high temperature exposure, depending on confining pressure and exposure times (Table 2). This drop in stiffness can be accompanied by a drop in failure strength of ~40%. Accordingly, in this temperature interval, support and protection of the casing by cement sheath can be significantly reduced, and well integrity may be jeopardized. Operation temperatures of 210-240°C are common for SAGD wells (Chartier et al., 2015), while operations temperatures may fluctuate between 25 and 340°C for CCS wells (Stiles, 2006). Accordingly, operation of these wells is in the temperature window for which the reduced stiffness and strength is observed, and well integrity will be affected by these changes in mechanical behavior. Some geothermal wells target super-hot reservoirs containing supercritical fluids, such as the IDDP-1 and IDDP-2 well (Iceland Deep Drilling Project) with envisaged reservoir temperatures and pressures reaching up to above 400°C and 300 bars (Friðleifsson et al., 2015). Long term exposure of well cement to temperatures above 400°C is expected for such wells. Wellbore integrity of these wells may be critically affected by changing mechanical properties of well cement between 120 and 250°C during thermal recovery after drilling. The cement may regain stiffness and strength after exposure at temperatures above ~400°C, but not if the cement is already severely fractured before reaching these conditions.

Important issues with loss of well integrity in high temperature wells are that cement damage leads to (1) fluid migration along the wells (i.e. casing-cement-rock interfaces) and through the cement sheath to the casing, and (2) reduced support of the casing to sustain mechanical loads. Fluid migration reduces thermal isolation of the casing by the cement sheath and enhances thermal stresses and corrosion. Higher mechanical loads on the casing will increase the risks of casing buckling and collapse. For the high temperature cement investigated in this study, a change in the mechanical behavior of the cement is observed from more brittle deformation at low confining pressures to more ductile deformation at high confining pressures with a considerable residual strength after exceeding the failure strength. It suggests that the cement may still support relatively large differential loads under high confinement, even after exceeding its failure strength. Accordingly, the experimental data in this study aid in the development new cement formulations with improved mechanical properties and in the design of operations for high temperature wells to mitigate cement damage. The main challenge in designing improved cement is to mitigate problematic changes in mechanical properties during exposure at high temperatures while maintaining low viscosity of cement slurry during well cementation. The data also provide valuable input for modeling studies that aim to assess critical conditions for loss of well integrity (Kaldal et al., 2016; TerHeege et al., 2018).

5. CONCLUSIONS

The relation between changes in mineralogy and mechanical properties of Dyckerhoff HT Basic Blend of cement clinker (API class G cement) with 40 % silica flour was investigated. Samples were exposed to temperatures of 60-420°C for different exposure times. The effect of mineralogical changes on mechanical properties was investigated using a combination of (1) chemical analysis using X-ray diffraction (XRD), (2) microstructural analysis using scanning electron microscopy (SEM) and optical microscopy, and (3) mechanical properties (failure and residual strength, Young's modulus) using triaxial strength tests at confining pressures of 2-15 MPa.

The following can be concluded:

- The relation between mineralogy, microstructure and mechanical behavior of synthetic cement samples is complex. Mineralogical changes occurring between curing at 60 and 120°C result in slightly stiffer and stronger cement. Cement becomes less stiff and weaker if temperatures are raised to 250°C, and stiffer and stronger if temperatures increase to 420°C for intact samples.
- The change in mechanical behavior is likely due to the combined effect of changing porosity, microstructure and strength of mineral phases. The most important mineralogical changes are the formation of stronger xonotlite and wollastonite phases with higher density at the expense of tobermorite, α-C_2S hydrate, afwillite,

brownmillerite and katoite, and changes in amorphous content. These mineralogical changes are accompanied by a change in porosity due the different volume of reaction products, and by changes in microstructure (e.g., voids filled with needle-shaped crystals).

- For all exposure times and temperatures, deformation of the cement is more brittle deformation at low confining pressures and more ductile deformation at high confining pressures. A considerable residual strength remains after exceeding the peak differential stress, and the cement may still carry large differential loads even after exceeding its failure strength.
- The integrity of high temperature wells used for steam assisted gravity drainage and cyclic steam stimulation is particular affected by the mineralogical, microstructural and mechanical changes as operation temperatures of these wells are in the same temperature window for which reduction in cement stiffness and strength is highest. Geothermal wells targeting super-hot reservoirs containing supercritical fluids may be critically affected by changing mechanical properties of well cement between 120 and 250°C during thermal recovery after drilling, but the cement may regain stiffness and strength after exposure at temperatures above ~400°C.

ACKNOWLEDGEMENTS

The work has been published as part of the GEOWELL project, funded by the European Union's Horizon 2020 research and innovation program under grant agreement number 654497.

REFERENCES

1. Al-Ajmi, A.M. and R.W. Zimmerman. 2005. Relation between the Mogi and the Coulomb failure criteria. *Int. J. Rock Mech. & Min. Sc.* 42: 431-439.
2. Chartier, M.A., S. Thompson, M. Bordieanu, G. Bustamante, R. Saunders, and T.M.V. Kaiser. 2015. Performance Characterization and Optimization of Cement Systems for Thermally Stimulated Wells. SPE-174493-MS.
3. Enform, 2012. *In Situ Heavy Oil Operations, An Industry Recommended Practice (IRP) for the Canadian Oil and Gas Industry*. Ed. 3.2. Drilling and Completion Committee (DACC).
4. Gabrovšek, R., B. Kurbus, D. Mueller, and W. Wieker. 1993. Tobermorite formation in the system CaO, $C_3SSiO_2Al_2O_3NaOHH_2O$ under hydrothermal conditions. *Cement and Concrete Research* 23: 321–328.
5. Friðleifsson, G.Ó., B. Pálsson, A.L. Albertsson, B. Stefánsson, E. Gunnlaugsson, J. Ketilsson, and Þ. Gíslason. 2015. IDDP-1 Drilled Into Magma – World's First Magma-EGS System Created. In *Proceedings World Geothermal Congress, Melbourne, Australia, 19-25 April 2015*.
6. Kaldal, G.S., M.T. Jonsson, H. Palsson, and S.N. Karlsdottir. 2016. Structural modeling of the casings in the IDDP-1 well: Load history analysis. *Geothermics* 62: 1-11.
7. Kovari, K., A. Tisa, H.H. Einstein, and J.A. Franklin. 1983 Suggested methods for determining the strength of rock materials in triaxial compression: Revised version. *Int. J. Rock Mech. Min. Sci. & Geomech. Abstr.* 20: 283–290.
8. Kyritsis, K., C. Hall, D.P. Bentz, N. Meller, and M.A. Wilson. 2009. Relationship between engineering properties, mineralogy, and microstructure in cement-based hydroceramic materials cured at 200 - 350 C. *Journal of the American Ceramic Society* 92: 694–701.
9. Meller, N., C. Hall, and J.S. Phipps. 2005. A new phase diagram for the CaO–Al2O3 –SiO2 –H2O hydroceramic system at 200°C. *Materials Research Bulletin* 40: 715–723.
10. Papaioannou, A. 2018. *Impact of in-situ ageing on the mineralogy and mechanical properties of Portland-based cement in geothermal applications*. M.Sc. thesis Utrecht University: 44 p.
11. Patchen, F.D. 1960. Reaction and Properties of Silica-Portland Cement Mixtures Cured at Elevated Temperatures. *Journal of the Society of Petroleum Engineers* 219: 281–287.
12. Pernites, R.B., and A.K. Santra. 2016. Portland cement solutions for ultra-high temperature wellbore applications. *Cement and Concrete Composites* 72: 89-103.
13. Stiles, D. 2006. Effects of Long-Term Exposure to Ultrahigh Temperature on the Mechanical Parameters of Cement. SPE-98896.
14. Taylor, H.F.W. 1990. *Cement chemistry*. Academic Press.
15. TerHeege, J.H., B. Orlic, and J. Wollenweber. Discrete element modelling of wellbore integrity in high temperature geothermal reservoirs. In *Proceedings of the 51st US Rock Mechanics / Geomechanics Symposium held in San Francisco, California, USA, 25-28 June 2017*. American Rock Mechanics Association (ARMA 17-176).
16. Thorvaldson, T. 1938. Portland Cement and Hydrothermal Re-actions. In *Symposium of the Chemistry of Cement, Stockholm.*